Study of the $Nd_{0.7}A_{0.3}Mn_{1-x}B_xO_3$ (A = Pb, Cd; B = Fe, Co, Ni; x = 0, 0.1) Phases: Synthesis, Characterization, and Magnetic Properties

J. J. Blanco,† L. Lezama,† M. Insausti,† J. Gutiérrez,‡ J. M. Barandiarán,‡ and T. Rojo*,†

Dptos. Química Inorgánica and Electricidad y Electrónica, Facultad de Ciencias, Universidad del País Vasco, Apdo. 644, E−48080 Bilbao, Spain

Received February 1, 1999. Revised Manuscript Received June 29, 1999

The $Nd_{0.7}A_{0.3}Mn_{1-x}B_xO_3$ (A = Pb, Cd; B = Fe, Co, Ni; x = 0, 0.1) compounds have been synthesized using the sol−gel method and characterized by redox titration and X-ray diffraction. The replacement of manganese ions by Fe, Co or Ni implies a decrease in the ferromagnetic (or metal−insulator) transition temperature. The ZFC magnetization drops to zero at low temperatures, showing a general weakening of the ferromagnetic DE interactions and an increasing contribution of the AFM ones arising by superexchange. Similar effects have been observed in the cadmium phases but substitutions of Fe, Co and Ni cations do not modify the magnetic behavior of these phases. The difference observed between the para-ferromagnetic transition temperature, T_c, and the metal−insulator one could be explained because of the appearance of magnetically inhomogeneous regions. Values of magnetoresistance around 70% for the lead compounds have been obtained. From ESR measurements at room temperature for all of the samples, different line widths related to the kind of metals present in the cell and the corresponding T_c have been obtained. The line width values are higher for the cadmium phases than those for the lead ones, and within each family, it increases as follows: Ni < Fe < Co.

Introduction

Studies on the structure−property relationships in the $Ln_{1-x}A_xMnO_3$ (Ln = La, Nd, Pr, Sm; A = Ca, Sr, Ba, Pb)[1] perovskites indicate the appearance of two families, depending on the average size of the interpolated cations. Compounds with large cations, such as the $Ln_{1-x}A_xMnO_3$ (Ln = La, Pr; A = Ca, Sr, Ba, Pb) oxides, exhibit a transition from a ferromagnetic metallic to a paramagnetic insulating state. The highest T_c values are obtained for larger Ln cations. For a given size of the lanthanide, the T_c values decrease with the Mn^{3+}/Mn^{4+} ratio.[2−4] It was considered that the mechanism for this transition lays in the double-exchange (DE) interaction,[5] but additional polaronic and Jahn−Teller effects have also been proposed to explain the magnetoresistance behavior.[6,7] On the contrary, manganites with small A cation such as $Ln_{0.5}Ca_{0.5}MnO_3$ (Ln = Pr, Nd, Sm) present a semiconducting behavior in the whole temperature range, being antiferromagnetic at low temperatures.[8,9,10] In fact, the small size of the substituted cations favors charge ordering hindering the metal−insulator (MI) transition.

An exhaustive study on the effects of the rare-earth displacement in the manganites has been carried out.[1−9] However, the influence of the substitution at the Mn sites for other elements is not well-known. The effect of trivalent (Cr^{3+}, Co^{3+}, Fe^{3+}, Al^{3+}, Ga^{3+}) and tetravalent (Ti^{4+}, Sn^{4+}) cations in La-, Pr-, and Sm-based compounds have recently been reported.[11] The introduction of nickel(II) ions in the $Ln_{0.5}Ca_{0.5}Mn_{1-x}Ni_xO_3$ (Ln = Pr, Nd, Sm) phases causes the disappearance of charge ordering inducing the metal−insulator transition.[12] The random distribution of the Al^{3+} cations in $La_{2/3}Ca_{1/3}Mn_{0.8}Al_{0.2}O_{3-\delta}$ ($x \leq 0.1$) generates values of magnetoresistance of 10^7% at H = 12T and low temperatures.[13] In the $Sm_{0.56}Sr_{0.44}Mn_{0.97}Fe_{0.03}O_3$ phase, an

* To whom all correspondence should be addressed. E-mail: qiproapt@lg.ehu.es. Fax: 34-94-4648500. Telephone: 34-94-6012458.

† Dpto. Química Inorgánica, Universidad del País Vasco.

‡ Dpto. Electricidad y Electrónica, Universidad del País Vasco.

(1) Coey, J. M. D.; Viret, M.; von Molnár, S. *Adv. Phys.* **1999**, *48* (2), 167.

(2) Caignaert, V.; Maignan, A.; Raveau, B. *Solid State Commun.* **1995**, *95*, 357.

(3) Maignan, A.; Simon, Ch.; Caignaert, V.; Raveau, B. *J. Mater. Chem.* **1995**, *5*, 1089; *Z. Phys. B* **1996**, *99*, 305.

(4) Hwang, H. Y.; Cheong, S. W.; Radaelli, P. G.; Marezio, M.; Baatlogg, B. *Phys. Rev. Lett.* **1995**, *75*, 914.

(5) Zener, C. *Phys. Rev.* **1951**, *82*, 403.

(6) Billinge, S. J. L.; DiFrancesco, R. G.; Kwei, G. H.; Neumeier, J. J.; Thompson, J. D. *Phys. Rev. Lett.* **1996**, *77*, 715.

(7) Millis, A. J.; Shraiman, B. I.; Mueller, R. *Phys. Rev. Lett.* **1996**, *77*, 175.

(8) Tomioka, Y.; Asamitsu, A.; Kuwahara, H.; Moritomo, Y. *Phys. Rev. B* **1996**, *53*, 1689.

(9) Woodward, P. M.; Vogt, T.; Cox, D. E.; Arulraj, A.; Rao, C. N. R.; Karen, P.; Cheetham, A. K. *Chem. Mater.* **1998**, *10*, 3652. Rao, C. N. R.; Arulraj, A.; Santosh, P. N.; Cheetham, A. K. *Chem. Mater.* **1998**, *10*, 2714.

(10) Vanitha, P. V.; Singh, R. S.; Natarajan, Sreenivisan; Rao, C. N. R. *J. Solid State Chem.* **1998**, *137*, 365. Martin, C.; Maignan, A.; Raveau, B. *J. Mater. Chem.* **1996**, *6* (7), 1245. Sugantha, M.; Singh, R. S.; Guha, A.; Raychaudhuri, A. K.; Rao, C. N. R. *Mater. Res. Bull.* **1998**, *33* (7), 1129.

(11) Damay, F.; Maignan, A.; Martin, C.; Raveau, B. *J. Appl. Phys.* **1997**, *82* (3), 1485.

(12) Maignan, A.; Damay, F.; Martin, C.; Raveau, B. *Mater. Res. Bull.* **1997**, *32* (7), 965.

10.1021/cm991014a CCC: $18.00
Published on Web 11/17/1999

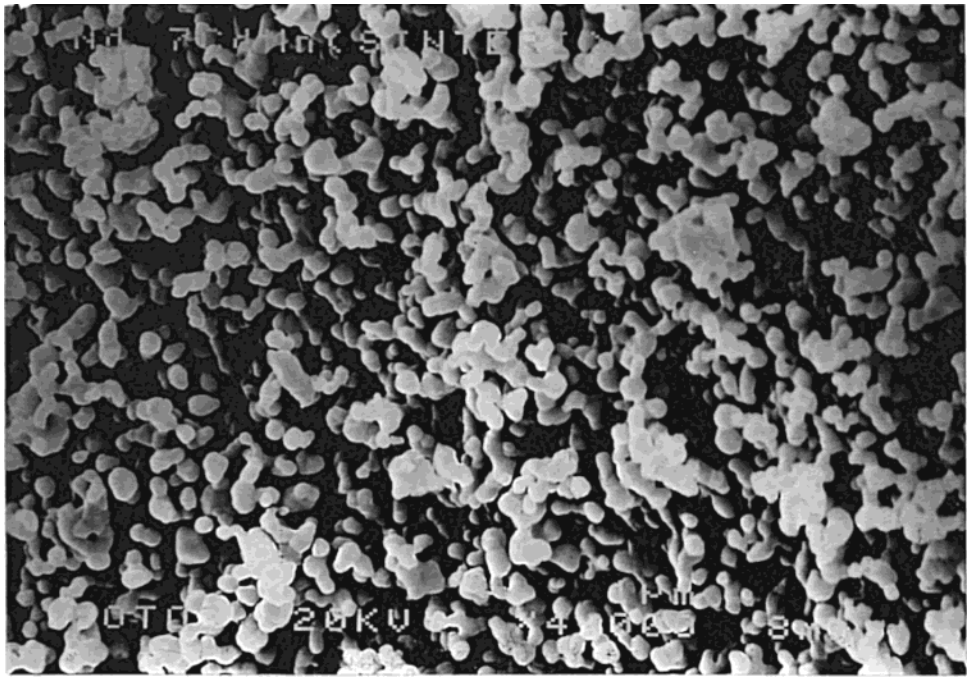

Figure 1. SEM photograph of the $Nd_{0.7}Cd_{0.3}MnO_3$ phase sinterized at 900 °C.

increase of the GMR ratio up to 10^6 by iron doping has been observed.[14]

In this paper, we present the synthesis and characterization of the $Nd_{0.7}A_{0.3}Mn_{1-x}B_xO_3$ (A = Pb, Cd; B = Fe, Co, Ni; $x = 0$, 0.1) phases in order to know the influence of both the A cations and the substitution in the Mn sites. The study of the magnetic and magnetoresistance properties allows one to clarify the behavior of the ferromagnetic metallic state arising from the double-exchange interaction when it is mixed with other different types of interactions.

Experimental Section

The $Nd_{0.7}A_{0.3}Mn_{1-x}B_xO_3$ (A = Pb, Cd; B = Fe, Co, Ni; $x = 0$, 0.1) compounds were prepared by the sol−gel method. Stoichiometric amounts of Nd_2O_3, $Pb(NO_3)_2$, $Cd(NO_3)_2$, $Mn(C_2H_3O_2)_2 \cdot 9H_2O$, FeO, NiO, or CoO were used as starting materials. An aqueous solution of citric acid was added to an aqueous solution of the metallic ions with the pH adjusted to 1.0 with nitric acid. After that, ethylene glycol was added. The gel obtained was dried at 100 °C in a sand bath and then fired at 773 and 1073 K for 10 h. The microcrystalline powder obtained was pelletized and sintered at 1173 K for 10 h in flowing oxygen.

The Mn^{3+}/Mn^{4+} ratio was determined by redox titration using an excess of $FeSO_4$ solution and back-titration with potassium permanganate. X-ray diffraction patterns were collected at room temperature on a STOE diffractometer using Cu $K\alpha_1$ radiation. Data were collected by scanning in the range $5° < 2\theta < 120°$ with increments of $0.02°(2\theta)$. The structures were refined by the Rietveld method using the FULLPROF program.[15] Magnetic and resistance measurements were performed in the temperature range 1.8−300 K using a Quantum Design MPMS-7 SQUID magnetometer. The magnetic measurements were performed at magnetic fields between 0 and 7 T. The resistance and magnetoresistance versus temperature measurements were carried out by means of a direct current four-probe system with the current parallel to the applied field. Electron paramagnetic resonance spectra were recorded on a Bruker ESP300 spectrometer, equipped with standard Oxford low-temperature devices operating at X band. The magnetic field was measured with a Bruker BNM 200 gaussmeter, and the frequency was determined by using a Hewlett-Packard 5352B microwave frequency counter. Scanning electron microscopic (SEM) observations were also carried out to give some indication of the oxide compactness using a JEOL JSM-6400 instrument.

Results

Structural Characterization. The $Nd_{0.7}A_{0.3}Mn_{1-x}B_xO_3$ (A = Pb, Cd; B = Fe, Co, Ni; $x = 0$, 0.1) compounds were synthesized as polycrystalline powders. The morphology of the obtained particles is shown in the SEM photograph of Figure 1, which corresponds to the synthesized pellets. The microstructure reveals uniform and fine grain growth, around 0.3 μm. The sol−gel process used in the synthesis of the compounds gives rise to the formation of small-size particles with a considerable degree of agglomeration, which can be attributed to the fineness of the grains. The substitution of neodymium for other divalent cations generates, in all cases, the oxidation from Mn^{3+} to Mn^{4+}, which is observed, by redox titration, to yield an amount of Mn^{4+} higher than that corresponding to the stoichiometric phase. This fact can be attributed to either an excess of oxygen or a defect of neodymium or manganese in the structure.[16]

All of the phases crystallize in the orthorhombic space group *Pnma* (D_{16}^h). The structure can be visualized as a distorted ideal cubic perovskite where distortions arise from displacements of oxygen and rare-earth atoms from ideal cubic positions. These kinds of distortions are produced by the different ionic radii of the atoms present in the structure and are related to the Goldsmith

(13) Blasco, J.; García, J.; de Teresa, J. M.; Ibarra, M. R.; Perez, J.; Algarabel, P. A.; Marquina, C.; Ritter, C. *Phys. Rev. B* **1997**, *55* (14), 8905.

(14) Damay, F.; Maignan, A.; Nguyen, N.; Raveau, B. *J. Solid State Chem.* **1996**, *124*, 385.

(15) Rodriguez-Carvajal, J. *Physica B* **1992**, *192*, 55.

(16) Cherepanov, V. A.; Barkhatova, L. Yu.; Petrov, A. N.; Vorinin, V. I. *J. Solid State Chem.* **1995**, *118*, 53.

Table 1. Selected Data Obtained from X-ray Diffraction Refinement at Room Temperature for the $Nd_{0.7}A_{0.3}Mn_{1-x}M_xO_3$[a] Compounds

sample		NdPbMn	NdPbMnFe	NdPbMnCo	NdPbMnNi
a[b]		5.4548(5)	5.463(2)	5.4597(7)	5.4556(6)
b[b]		7.7075(6)	7.725(4)	7.714(1)	7.6999(7)
c[b]		5.4835(5)	5.485(3)	5.470(1)	5.4776(6)
V[c]		230.54	231.48	230.38	230.10
Mn−O(1)[b]	2	1.98(1)	1.977(9)	1.966(7)	1.938(5)
Mn−O(2)[b]	2	1.99(5)	2.03(3)	1.96(3)	1.94(4)
[b]	2	1.91(6)	1.89(3)	1.95(3)	1.97(4)
Mn−O(1)−Mn[d]	2	153(2)	156(2)	157(2)	166(3)
Mn−O(2)−Mn[d]	4	164(1)	162(2)	163(2)	161(2)
sample		NdCdMn	NdCdMnFe	NdCdMnCo	NdCdMnNi
a[b]		5.4038(4)	5.4325(6)	5.4256(3)	5.4208(3)
b[b]		7.6840(5)	7.6959(7)	7.6843(4)	7.6779(4)
c[b]		5.4224(4)	5.4092(5)	5.3994(3)	5.3978(4)
V[c]		225.15	226.14	225.11	224.66
Mn−O(1)[b]	2	2.00(1)	1.962(9)	1.953(4)	1.962(6)
Mn−O(2)[b]	2	1.98(4)	2.08(4)	1.97(2)	2.06(2)
[b]	2	1.91(4)	1.85(4)	1.95(2)	1.84(2)
Mn−O(1)−Mn[d]	2	146(3)	157(3)	159(1)	156(2)
Mn−O(2)−Mn[d]	4	159(2)	153(2)	154(1)	156(1)

[a] A = Pb, Cd; M = Fe, Co, Ni; $x = 0, 0.1$. [b] In angstroms. [c] In cubic angstroms. [d] In degrees.

tolerance factor,[17] defined for a ABO_3 perovskite as $t = (r_A + r_O)/(r_B + r_O)(2)^{1/2}$. Higher tolerance factors have been found for the lead compounds ($t = 0.97$) than those for the cadmium ones ($t = 0.95$). However, the values are always lower than the ideal $t = 1$. This fact indicates that the octahedral tilt in the phase around the (1 1 0) and (0 0 1) directions giving rise to an orthorhombic unit cell. Table 1 summarizes the relevant structural parameters obtained by Rietveld analysis of the diffractograms. Unit cell parameters reduce gradually when substituting Pb^{2+} by Cd^{2+}, in good accordance with the lower ionic radii. The substitution for iron, cobalt or nickel ions does not affect greatly the cell parameters because of the similarity in the ionic radii. Another important aspect to be considered is the configuration of the MnO_6 octahedra in the different compounds. As can be seen in Table 1, two different values are observed in the Mn−O distances ranging from 1.84(2) to 2.06(2) Å. Taking into account that a lengthening of two of the Mn−O bonds is not observed, it can be deduced that the cooperative Jahn−Teller lattice distortions are either frustrated or must adopt new ordered arrangements. In the case of the cadmium compounds, the decrease in the tolerance factor generates a distortion in the unit cell, which would lead to the zigzag of octahedra containing the manganese atoms.[18] The Mn−O−Mn angles are smaller than those observed in the lead compounds being a key factor in the control of the Mn−Mn electronic hopping.[19]

Magnetic and Transport Properties. The temperature dependence of the FC and ZFC magnetizations for some of the phases is shown in Figure 2. The observed T_c values, obtained as the minimum of the curve dM/dT calculated from the measured ZFC curves, are given in Table 2. In the case of the lead phases, the T_c in the parent compound, $Nd_{0.7}Pb_{0.3}MnO_3$, is 175 K and gradually decreases to lower temperatures when

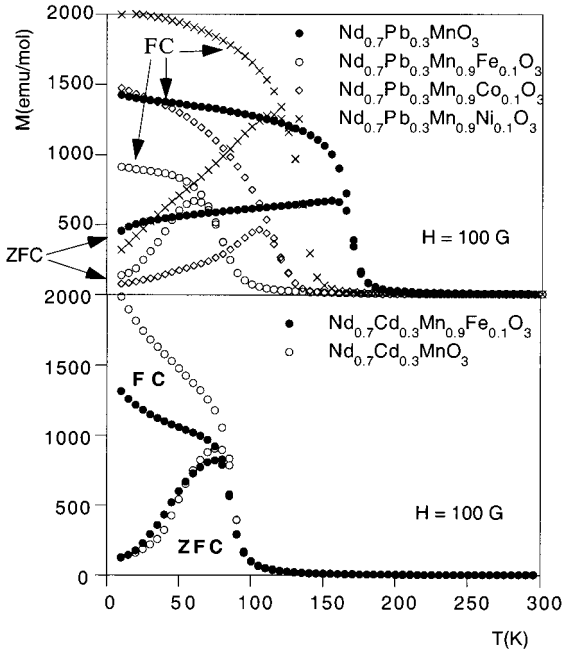

Figure 2. Thermal evolution of the magnetization (field cooling, FC, and zero field cooling, ZFC) for (a) Nd−Pb and (b) Nd−Cd phases.

Mn is replaced by Ni, Co, and Fe. In the case of the cadmium phases, the T_c is 90 K. No changes were observed in the Co- and Ni-substituted phases. The values of the effective magnetic moments, μ_{eff} (determined from the χ^{-1} curves), together with the calculated ones ($\mu_t = (x\mu^2_{Mn} + (1 - x)\mu^2_M)^{1/2}$) have also been included in Table 2. The smaller values observed in all cases for the μ_{eff} (calcd) indicate that a compensation of the spins is being carried out when manganese is replaced by other ions. From the form of the curve in Figure 2, it can be deduced that for the $Nd_{0.7}Pb_{0.3}MnO_3$ phase the M_{ZFC} curve for $T < T_c$ is almost independent of temperature. In this way, the local clustering of the Mn^{3+} ions at around the Mn^{4+} ones eventually leads to a ferromagnetic order of long-range type. On the contrary, M_{ZFC} of the substituted phases decreases significantly on cooling below T_c.

(17) Goldsmith, V. M. *Geochemische Verteilungsgesetze der Elemente VII−VIII*; 1928.
(18) Cho, J. H.; Park, I. K.; Kim, H. G.; Chung, H. T. *J. Am. Ceram. Soc.* **1997**, *80* (6), 1523.
(19) Attfield, J. P. *Chem. Mater.* **1998**, *10*, 3239.

Table 2. Values of Curie Temperatures (T_c), Theoretic Magnetic Moments ($\mu_{eff}(t)$) and Calculated from Cm Values (μ_{eff}(exp)) and Peak-to-Peak Line Width, ΔH_{pp} (G), for the $Nd_{0.7}A_{0.3}Mn_{1-x}M_xO_3$[a] Compounds

	$\mu_{eff}(t)$ μ_B	μ_{eff}(exp) μ_B	T_c (K)	ΔH_{pp} (G)
$Nd_{0.7}Pb_{0.3}MnO_3$	6.30	6.58	175	1015
$Nd_{0.7}Pb_{0.3}Mn_{0.9}Fe_{0.1}O_3$	6.15	5.84	80	2001
$Nd_{0.7}Pb_{0.3}Mn_{0.9}Co_{0.1}O_3$	6.11	5.04	110	>7000
$Nd_{0.7}Pb_{0.3}Mn_{0.9}Ni_{0.1}O_3$	6.01	5.41	140	1286
$Nd_{0.7}Cd_{0.3}MnO_3$	6.30	6.08	90	2945
$Nd_{0.7}Cd_{0.3}Mn_{0.9}Fe_{0.1}O_3$	6.15	5.80	90	3646
$Nd_{0.7}Cd_{0.3}Mn_{0.9}Co_{0.1}O_3$				>7000
$Nd_{0.7}Cd_{0.3}Mn_{0.9}Ni_{0.1}O_3$				2988

[a] A = Pb, Cd; M = Fe, Co, Ni; x = 0, 0.1.

Resistivity measurements have been carried out at zero-field and 6 T. The results for the $Nd_{0.7}Pb_{0.3}MnO_3$ and $Nd_{0.7}Pb_{0.3}Mn_{0.9}Ni_{0.1}O_3$ phases, considered as representative, are shown in Figure 3. The $Nd_{0.7}Pb_{0.3}MnO_3$ phase exhibits a transition from a metallic to a semiconducting state with increasing temperature. With application of the magnetic field, the resistivity decreases, reaching maximum values of magnetoresistance around 70%. For the $Nd_{0.7}Pb_{0.3}Mn_{0.9}Ni_{0.1}O_3$ compound, a maximum is not observed at 0 T, with the sample remaining an insulator up to 50 K, where the resistivity is too high to be measured. Nevertheless, when a magnetic field of 6 T is applied, the resistivity decreases and a maximum at 75 K is visualized. The magnetoresistance values calculated for the other compounds are also around 70%. This fact indicates that the presence of other cations such as cobalt does not have any influence in the magnetoresistive values.

ESR Spectroscopy. The powdered X band electron paramagnetic resonance spectra corresponding to the paramagnetic region of the samples are given in Figure 4. Isotropic broad signals with $g \approx 2$ appear for all the phases. The line widths observed in the spectra are on the same order of magnitude as those found in manganites incorporating rare-earth ions (ΔH = 2000 Oe).[20] In absence of strong exchange interactions, the line width is caused by the random dipolar field from both the Mn and Nd ions. Nevertheless, some differences have been observed in the values of the line widths for the different phases (Table 2). These changes would be related to both the kind of metallic ions present in the cell and the corresponding T_c for each compound. The values for the cadmium phases are higher than those of the lead ones, and within each family, the values increase as follows: Ni < Fe < Co.

In the case of the $Nd_{0.7}Pb_{0.3}MnO_3$ and $Nd_{0.7}Cd_{0.3}MnO_3$ compounds, ESR measurements below and above T_c have also been performed. The spectra corresponding to the $Nd_{0.7}Cd_{0.3}MnO_3$ phase appear in Figure 5. The peak to peak line width and the values of the magnetic field for which the absorption is maximum at different temperatures have been represented in Figure 6. Lorentzian line shape curves have been observed for the spectra above T_c. The signal obtained at 110 K, which is fitted to a Lorentzian function, is represented by a discontinuous line in Figure 5, showing a good accordance. Nevertheless, the line width decreases with

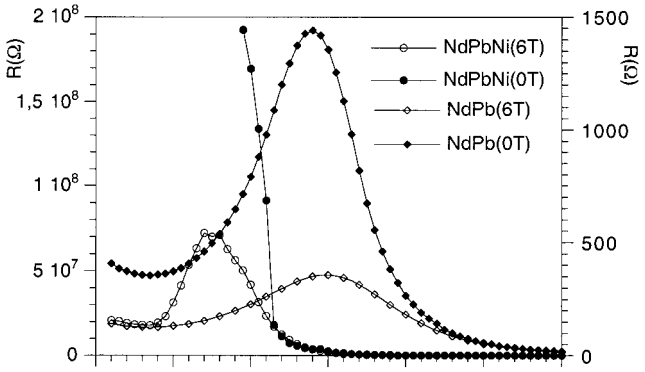

Figure 3. Temperature variation of the resistivity for the $Nd_{0.7}Pb_{0.3}MnO_3$ and $Nd_{0.7}Pb_{0.3}Mn_{0.9}Ni_{0.1}O_3$ phases.

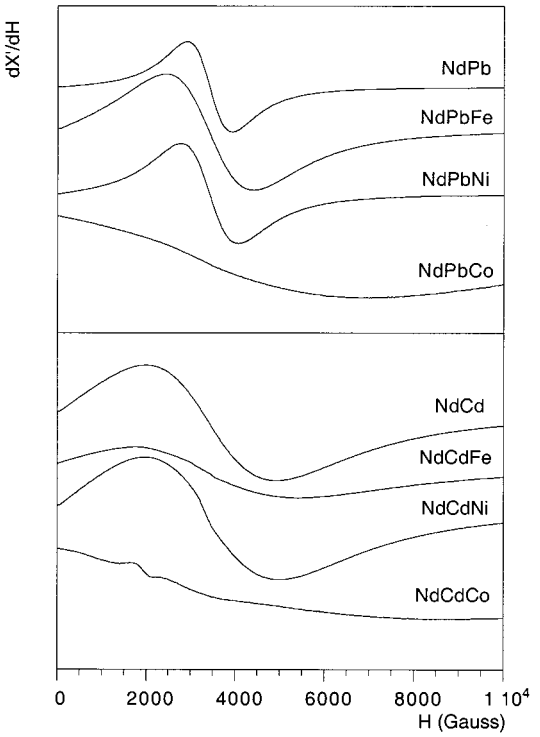

Figure 4. X band ESR spectra at room temperature for the $Nd_{0.7}A_{0.3}Mn_{1-x}B_xO_3$ (A = Pb, Cd; B = Fe, Co, Ni; x = 0, 0.1) phases.

decreasing temperature, reaching a minimum value near the Curie point (see Figure 6). This effect could be explained by the exchange-narrowed spin−spin interaction together with the increasing of the spin−lattice relaxation time. At lower temperatures, the line width increases when the temperature decreases, showing the characteristics of a Dyson line, the typical shape of a metallic state.[21] Below the temperature of the magnetic transition, a change in the conducting properties appears.

It is interesting to note that in the case of the $Nd_{0.7}Pb_{0.3}MnO_3$ phase an almost linear dependence of ΔH_{pp} versus T has been found from 145 to 300 K, in good agreement with the results described in the literature for other La-based manganites.[22,23] Concerning the magnetic field for which the absorption is maximum, there is a slight variation of the resonant field with temperature between 290 and 170 K, being the value

(20) Rubinstein, M.; Gillespie, D. J.; Snydeer, J. E.; Tritt, T. M. *Phys. Rev. B* **1997**, *56* (9), 5412.

(21) Dyson, F. *Phys. Rev.* **1955**, *98*, 349.

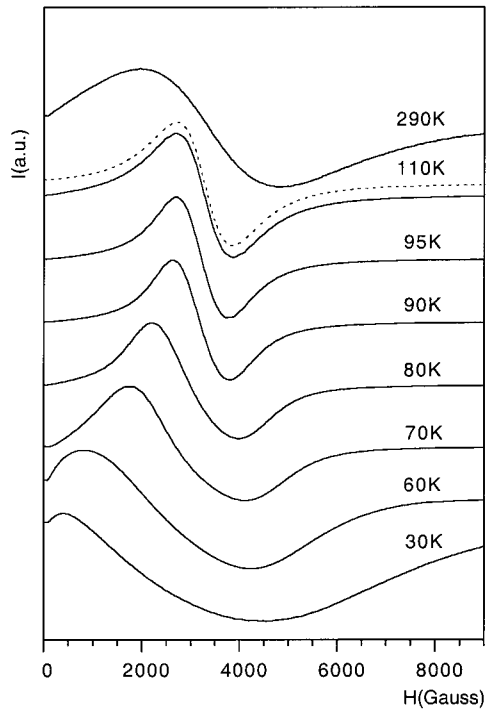

Figure 5. ESR measurements below and above T_c for the $Nd_{0.7}Cd_{0.3}MnO_3$ phase. The fitting to a Lorentzian function for the 110K signal is represented by the dotted (···) line.

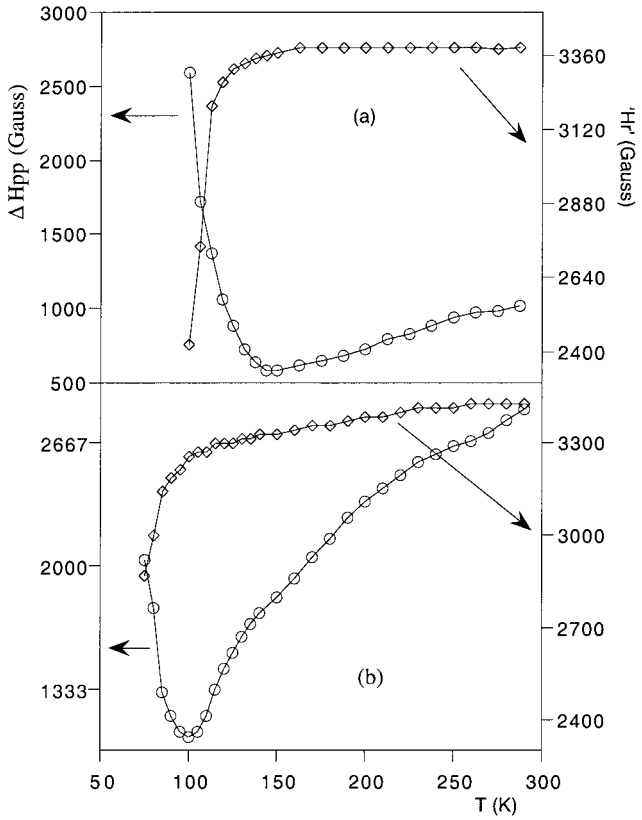

Figure 6. Thermal evolution of the line width (ΔH_{pp}) and the resonance field (Hr) for the (a) $Nd_{0.7}Pb_{0.3}MnO_3$ and (b) $Nd_{0.7}Cd_{0.3}MnO_3$ phases.

obtained for the *g* factor of 2.03 at 170 K.[22] Below that temperature an abrupt variation of the resonance field is observed. In this case, the resonance field cannot be related to the *g* factor, as the curve shows the characteristics of a Dyson line. For the $Nd_{0.7}Cd_{0.3}MnO_3$ phase,

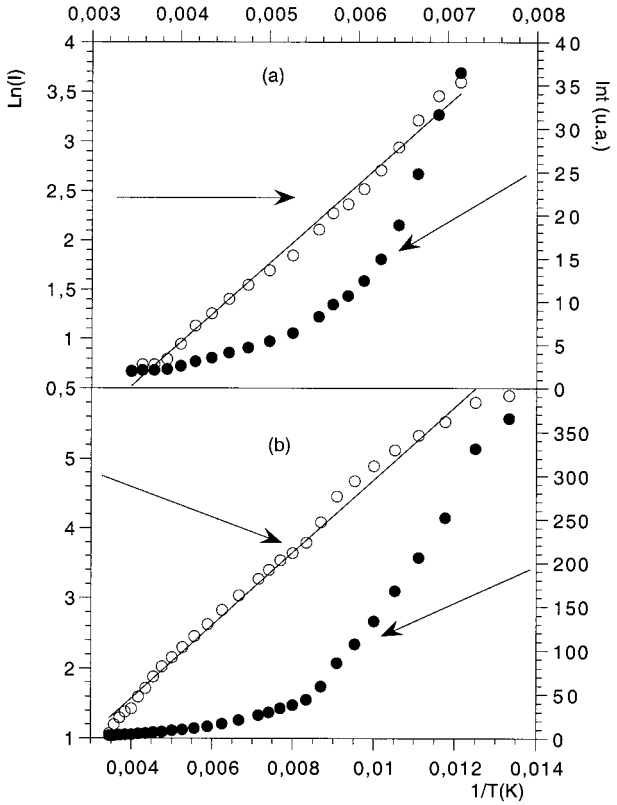

Figure 7. Thermal evolution of the intensity and the ln(*I*) for the (a) $Nd_{0.7}Pb_{0.3}MnO_3$ and (b) $Nd_{0.7}Cd_{0.3}MnO_3$ phases.

the line width does not decrease linearly with decreasing temperature, and, furthermore a significant variation of the resonant field with temperature can be observed between 300 and 100 K.

For the $Nd_{0.7}Pb_{0.3}MnO_3$ and $Nd_{0.7}Cd_{0.3}MnO_3$ compounds, the intensity of the resonance line at each temperature has been obtained from the normalized double integral of the $d\chi''/dH$ signal and is represented in Figure 7. The thermal evolution of the intensity can only be well fitted near room temperature by the following Arrhenius equation:

$$I = I_o \exp(\Delta E/k_B T)$$

where I_o is a fitting parameter, ΔE is a thermal activation energy for dissociation of magnetic interactions, and k_B is the Boltzmann constant. The best fits in the range 145−250 K for $Nd_{0.7}Pb_{0.3}MnO_3$ and 250−90 K for $Nd_{0.7}Cd_{0.3}MnO_3$ lead to the parameters ΔE = 801.2 and ΔE = 555.9 K, respectively (see Figure 7).

Discussion and Conclusions

The systematic study of the magnetic and transport properties in the $Nd_{0.7}A_{0.3}Mn_{1-x}B_xO_3$ (A = Pb, Cd; B = Fe, Co, Ni; x = 0, 0.1) compounds shows that the substitutions of Fe, Co, and Ni for Mn generate a large drop in the Curie temperatures. This effect is similar

(22) Oseroff, S. B.; Torikachvili, M.; Singley, J.; Ali, S.; Cheong, S.-W.; Schultz, S. *Phys. Rev. B* **1996**, *53* (10), 6521. Lofland, S. E.; Kim, P.; Dahiroct, P.; Bhagat, S. M.; Tyagi, S. D.; Karabashev, S. G.; Shulyater, D. A.; Arsenov, A. A.; Mukovskii, Y. *Phys. Lett.* **1997**, *A233*, 476.

(23) Shames, A. I.; Rozenberg, E.; Gorodetsky, G.; Pelleg, J.; Chaudhuri, B. K. *Solid State Comm.* **1998**, *107* (3), 91.

to that observed by other authors[10,24] and can be explained by a general weakening of the ferromagnetic DE interactions and an increasing contribution of the AFM ones arising from superexchange. In the case of the cadmium compound, the constant value of 90 K for the T_c could be interpreted on the basis of Mn−O−Mn bond angles for these phases smaller than that corresponding to the lead ones. This fact would not favor the transfer integral between Mn ions because of the inability of an itinerant electron to hop or tunnel without assistance from a manganese ion to a neighboring Fe, Co, or Ni ion.[10,25] The drop of the M_{ZFC} curve for $T < T_c$ values could be explained on the basis of a cluster glass type, as was previously observed in related phases.[26]

The values observed for the para-ferromagnetic transition temperature, T_c, and the metal−insulator one, T_{MI}, (see Table 2), which usually occur simultaneously,[3] show some differences. These can be attributed to the appearance of magnetically inhomogeneous regions in the samples, modifying the transport properties. This inhomogeneity could appear because of the presence of a higher content of vacancies (as can be deduced from the Mn^{3+}/Mn^{4+} ratio), which would be more pronounced in the case of the phases with either cadmium-substituting neodymium or iron, cobalt, and nickel-substituting manganese. Nevertheless, the use of soft synthesis conditions could also generate poorly crystallized ceramics where the peak in the resistivity lies at a temperature somewhat below T_c.[27]

In the case of the ESR spectra, the differences observed in the line widths could be due to two important facts. First, the resonances are all observed above the Curie temperature, which is different for each compound, and second, the cations used in the substitutions of the manganese ion are also different. It is worth mentioning that in the case of the lead phases, the smaller line width values correspond to the higher T_c. The presence of the Fe, Co, and Ni ions weakens the exchange field, as determined by the decrease in the Curie temperature, and accordingly, the line width increases. In the case of the cobalt phases, the broadening effect could be explained as due to the rapid spin−lattice relaxation of the Co ion. Nevertheless, in the case of the cadmium phases, where a change in the line width is also observed, the T_c temperatures are nearly independent of the substitutions of the metals, being in all cases around 90 K. From these results, it can be deduced that a decrease in the T_c values with the substitution of Mn for Ni, Co, or Fe should be observed. In this way, the similarity in the T_c for the cadmium phases could be attributed to changes in the sign of the predominant magnetic interactions produced from some structural changes. Further experiments at low temperatures should be performed in order to explain this fact.

The variation of the line width and resonant field with temperature for the $Nd_{0.7}Cd_{0.3}MnO_3$ phase could be explained as due to a progressive contraction of the crystallographic cell when decreasing the temperature. In this way, the presence of cadmium in these compounds would generate a continuous distortion in the cell or even a structural transition phase, giving rise to changes in the sign of the magnetic interactions. These changes favor the antiferromagnetic interactions against the ferromagnetic ones. Furthermore, this fact could also explain the appearance of an antiferromagnetic ordering at low temperatures in the magnetic measurements.

The evolution of the intensity of the resonance line with temperature in the studied phases can be explained as due to a short-range ordering among the spin-polarized carriers, with E_a being the activation energy needed for the dissociation of the clusters. This effect was also observed for other manganite phases, such as $La_{1-x}Ca_xMnO_{3+\delta}$,[28] in which the activation energies depend directly on the Mn^{3+}/Mn^{4+} ratio. These activation energies are on the same order as those obtained for the $Nd_{0.7}Pb_{0.3}MnO_3$ and $Nd_{0.7}Cd_{0.3}MnO_3$ compounds.

Finally, it is worthy of mention that both the control and the amount of the manganese substituted allow one to regulate the T_c values of the manganite phases, which is of great interest in the technological applications of these materials.

Acknowledgment. This work has been carried out with the financial support of the Ministerio de Educación y Ciencia (DGICYT PB94-0469 and PB97-0622 Grants) and Gobierno Vasco (PI9640), which we gratefully acknowledge.

CM991014A

(24) Sánchez, M. C.; Blasco, J.; García, J.; Stankiewicz, J.; de Teresa, J. M.; Ibarra, C. *J Solid. State Chem* **1998**, *138*, 226.
(25) Blasco, J.; García, J.; de Teresa, J. M.; Ibarra, M. R.; Algarabel, P. A.; Marquina, C. *J Phys. Condens. Matter.* **1996**, *8*, 7427.
(26) Itoh, M.; Natori, I.; Kubota, S.; Motya, K. *J. Phys. Soc. Jpn.* **1994**, *63*, 1486.
(27) Mahesh, R.; Mahendiran, R.; Raychaudhuri, A. K.; Rao, C. N. R. *J. Solid State Chem.* **1996**, *120*, 204. Mahendiran, R.; Mahesh, R.; Raychaudhuri, A. K.; Rao, C. N. R. *Solid State Commun.* **1996**, *99*, 149.
(28) Stasz, J. *Phys. Status Solidi* **1978**, *A47*, K23.